Evaluation and Life Extension of Asphalt Pavements Using Rejuvenators and Noncollinear Ultrasonic Wave Mixing: A Review

Megan E. McGovern
Manufacturing Systems Research Lab,
General Motors Research and Development,
30500 Mound Road,
Warren, MI 48092
e-mail: megan.mcgovern@gm.com

William Buttlar
Department of Civil and Environmental Engineering,
University of Missouri,
E2506 Lafferre Hall,
Columbia, MO 65211
e-mail: buttlarw@missouri.edu

Henrique Reis[1]
Department of Industrial and Enterprise Systems Engineering,
University of Illinois at Urbana-Champaign,
117 Transportation building,
104 S. Mathews,
Urbana, IL 61801
e-mails: h-reis@uiuc.edu; h-reis@illinois.edu

Except for the relatively small zones within pavements that are subjected to loadings, the primary challenge in asphalt concrete (AC) pavement design and maintenance is to prevent and/or control environmentally induced distresses. Distresses, including block and thermal cracking, and possibly raveling of construction joints, tend to accelerate with time; as a result, it is critical to evaluate the state of crack resistance in asphalt pavement surfaces before and after maintenance treatments. A review of the use of noncollinear wave mixing to evaluate oxidative aging of AC pavements, and the used of rejuvenators in oxidized pavements toward extension of pavement life, is presented. The approach requires no core extraction. Results show that the noncollinear wave mixing can evaluate the state of oxidative aging of AC pavements. Results also indicate that the use of rejuvenators is a successful strategy of pavement maintenance and sustainability.
[DOI: 10.1115/1.4037502]

Keywords: oxidative aging, asphalt concrete, noncollinear wave mixing, ultrasound, acoustic emission

1 Introduction

The inevitable aging of transportation infrastructure is continuously at odds with economic means to preserve the integrity and rideability of such infrastructure. Asphalt concrete (AC) pavements, in particular, are prone to deterioration via aging effects. In addition to traffic loads, exposure to harsh environmental elements during service, such as weather and oxygen, results in premature pavement failure by way of cracks, raveling, rutting, etc. Oxidation, caused by exposure to oxygen, is a particularly damaging mechanism because it causes the mastic to become weaker and more brittle, which significantly reduces its fracture performance (especially at low temperatures). Effects of oxidation are greatest at the top surface of the pavement, where exposure to oxygen is the greatest, and decrease with pavement depth. Although the chemical effects of oxidation on asphalt mastic are complex [1], it is widely accepted that the asphaltenes-to-maltenes ratio is a good measure of the oxidation level. An increase in the ratio indicates an increase in oxidation. This ratio change is due to a loss of volatile components during the aging process, a process which is accelerated by oxygen.

Pavement engineers are faced with the task of identifying this pavement damage and making cost-conscious decisions on the frequency and type of maintenance to perform. Preventative maintenance, when performed at the appropriate time, can significantly increase the life of pavements as well as save money in the long run. If maintenance is delayed too long, however, the costs to repair the pavement rapidly increase, as a much damaged pavement costs more to repair than a slightly damaged one. Furthermore, this effect is compounded: damaged pavements experience increasing amounts of damage in an accelerated manner. For example, cracks allow the infiltration of moisture into the pavements, which causes further damage during cold weather. Currently, pavement engineers have insufficient tools and resources with which to extend pavement life and to reduce maintenance and operations costs.

This report serves as a review of work performed and aims to demonstrate that the use of rejuvenators is a viable and cost-effective solution to combat the deterioration of aging roadways and airfield pavements. In particular, it will be demonstrated that asphalt rejuvenators, in combination with nonlinear acoustics, a nondestructive testing technique, which can rapidly, accurately, and nondestructively assess the pavement's "age," have the potential to address the deterioration due to oxidation, and extend pavements' life, thereby minimizing effort and costs. By monitoring and maintaining the pavement surface condition, damaging thermal and block cracks in asphalt concrete pavements can be minimized or altogether prevented.

The used nonlinear acoustic approach, in the form of a noncollinear wave mixing technique, involves the mixing of two ultrasonic waves to produce a third, nonlinear scattered wave. The characteristics of this third wave can be used to assess the oxidation level in the pavement, because the nonlinear acoustic properties of the pavement change with the level of oxidation. Specifically, two metrics are used to assess the pavement's oxidative age: (1) the frequency of interaction of the two primary waves and (2) the efficiency at which the third wave is generated. This technique is appealing, because it can be implemented in a truly nondestructive fashion via the use of critically refracted subsurface waves (that propagate close to and parallel to the surface), which enable one-sided pavement quality assessment.

2 Assessment of Oxidative Aging in Pavements

To address the need for a nondestructive method capable of quantifiably assessing the oxidation level of asphalt concrete pavements, a series of studies was carried out. The work in these studies followed a natural trajectory, starting with an investigation

[1]Corresponding author.

Manuscript received May 7, 2017; final manuscript received July 18, 2017. Editor: Tribikram Kundu.

of the effects of oxidation on the linear acoustic properties (i.e., velocities and attenuations) of AC [2,3]. In this study, it was recognized that oxidation results in the development of a diffuse microflaw population. Since nonlinear acoustic techniques are inherently more sensitive to damage, a nonlinear acoustic technique, in the form of noncollinear wave mixing, was thus employed. First, a feasibility study was performed [4], where samples were cut to the appropriate geometry to allow for incident mounting of the transducers for bulk wave mixing. The nonlinear acoustic technique was then extended to be applicable for field use by modifying the setup to be one sided [5] so that all measurements could be taken from the pavement surface. This was done by mounting the transducers on variable angle wedges to generate and mix subsurface waves. Two methods were introduced to determine the appropriate incident angle, when no linear acoustic properties are known a priori [6,7]. A *damage characterization curve* was introduced, whereby practitioners can determine the oxidative aging level of a pavement based on nonlinear acoustic measurements. Finally, the results were related to fracture performance properties of the aged AC specimens. Thus, Secs. 3 and 4 concern the development of the noncollinear wave mixing setup as a means to assess oxidative aging in AC pavements. The major results and conclusions from these investigations will now be reviewed/summarized in these sections. To conserve space, some details are omitted and only the fundamental background theory will be presented. For more details regarding experimental setups, etc., the reader is encouraged to refer to the appropriate citations.

3 Materials and Methods

Asphalt mixtures with 19 mm nominal maximum aggregate size and a target asphalt content of 5.9% (by weight of the total mixture), using PG64-22 as the base binder, were utilized. The blend percentages of aggregate blend used in asphalt mixture preparation consisting of four different stockpiles are: 65.3% coarse (CM16), 23% manufactured dolomite sand (FM20), 10.5% natural sand (FM02), and 1.2% mineral filler (MF).

Mixing of asphalt concrete mixtures was conducted at 155 °C using a standard bucket mixing procedure. Prepared loose asphalt mixtures were laboratory aged in an uncompacted condition for 0, 12, 24, 28, 32, and 36 h at 135 °C. Laboratory aging of the asphalt mixtures was performed by placing loose mixtures in a force draft oven (at 135 °C) for the appropriate amount of time (0–36 h). To ensure uniform aging throughout the sample, the mixtures were hand-stirred every 12 h.

3.1 Linear Acoustics. Prior to taking nonlinear acoustic measurements, a set of linear acoustic measurements were performed [2,3]. Here, the primary goal was to assess the effects of laboratory induced oxidative aging upon the ultrasonic velocities and attenuations of asphalt concrete mixtures. Through-transmission measurements were taken on the set of aged AC specimens to obtain the ultrasonic velocities and corresponding attenuations. For details on the experimental setup, the reader is referred to Refs. [2] and [3].

Figure 1 contains the average (across the measured frequency band) of the velocities and attenuations versus the level of laboratory oxidative aging. The velocity increases from 0 to 24 h and decreases with increasing aging after 24 h. Similarly, the attenuation decreases from 0 to 24 h, after which it increases with increasing aging. Based on this trend, a *critical aging point* was observed and identified, where once the aging level surpasses this point, damage rapidly accumulates. This trend was consistent with results from acoustic emission (AE) and complex moduli studies [3], and disk-shaped compact tension (DC(T)) fracture test [8].

To understand this trend, it is necessary to consider the physical phenomena occurring as the AC undergoes oxidation. As the mastic undergoes oxidation, the asphaltenes-to-maltenes ratio increases, which results in two major changes in the material properties: (1) mastic stiffness increases with oxidation and (2) the cohesive strength of the mastic as well as mastic-aggregate adhesion decreases. For the second mechanism, it results in decreased adhesion between the aggregates and mastic (so that flaws will appear at the aggregate-mastic interface rather than within the mastic). At low aging levels, the first mechanism dominates the global composite, i.e., the asphalt mixture, and therefore its material properties. At higher aging levels, the second mechanism dominates the global properties. The point at which the material properties transition from being dominated by the first mechanism to the second mechanism has been termed the *critical point*. From the linear acoustic measurements, this point was identified as 24 h of laboratory oxidative aging for that particular mixture, and it appears that is the point when the mixture loses its self-healing ability. Once the oxidation level surpasses the critical point, the adhesive strength loss dominates, which results in a drastic accumulation of microflaws. These microflaws result in an apparent reduction of the overall composite stiffness for aging levels beyond the critical point. In ultrasonic measurements, this results in lower ultrasonic dilatational and shear velocities (velocity is directly proportional to the stiffness) and higher ultrasonic attenuations.

3.2 Noncollinear Wave Mixing. The third-order nonlinear acoustic equations of motion were first developed by Murnaghan [9] in 1951, and then by Landau and Lifshitz [10] in 1954. Both derived the third-order nonlinear equations of motion and proposed a different set of third-order elastic constants (which are linear combinations of each other). The development of these equations of motion paved the way for noncollinear wave mixing, a nonlinear acoustic technique. Here, the technique will be discussed at a level sufficient to understand the fundamental background theory; however, the reader is referred to Refs. [11–20] for more comprehensive theory behind noncollinear wave mixing.

The noncollinear wave mixing approach was implemented to assess the oxidative aging in asphalt concrete materials. In this technique, two monochromatic ultrasonic waves with frequencies f_1 and f_2 are propagated so that they cross paths, see Fig. 2. In materials that are nonlinear in their constitutive behavior, these two waves can interact to produce a third wave, with a frequency of either $f_3 = f_1 \pm f_2$, termed the nonlinear scattered wave. Thus, one can imagine 54 various potential interaction scenarios when considering that the primary and scattered waves may be either (or all) dilatational waves, shear waves polarized in the interaction plane, or shear waves polarized out of the interaction plane. Out of 54 possible interaction cases, only ten satisfy the necessary resonant and polarization conditions [11–20] to make interaction possible. The relationships among the wave numbers and frequencies are most generally described as

$$k_3 = k_1 \pm k_2 \tag{1}$$

$$\omega_3 = \omega_1 \pm \omega_2 \tag{2}$$

where ω is the circular frequency ($\omega = 2\pi f$), and $\boldsymbol{k}$ is the wave vector ($|\boldsymbol{k}| = \omega/c$); by definition, $\omega_2 < \omega_1$. The nonlinear wave is separated from the two primary interacting waves in its mode, time-of-flight, direction, and frequency. The separation between the nonlinear scattered wave and the primary waves deem this method advantageous over other nonlinear acoustic methods, such as harmonic generation. The efficiency of the wave interaction (which can be quantified by the amplitude of the nonlinear scattered wave) and the frequency at which this interaction occurs will change with a change in material properties, i.e., linear acoustic velocity and attenuation, and nonlinear elastic behavior. The presence of microflaws, which are directly related to the oxidation level in asphalt mixtures, changes the nonlinear material behavior. As a result, it is natural to use noncollinear wave mixing as a means to detect oxidative aging level in asphalt concrete. The feasibility of using noncollinear wave mixing of subsurface

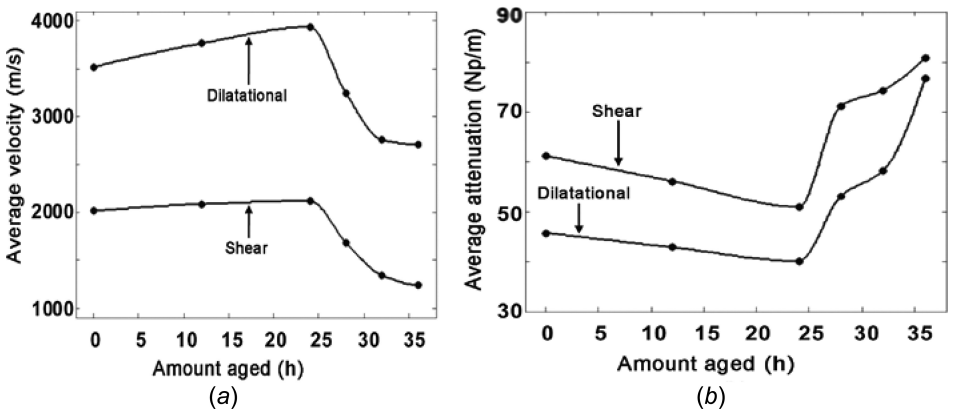

Fig. 1 Average across frequency of (*a*) velocities and (*b*) corresponding attenuations for AC samples aged 0–36 h (Reproduced with permission from McGovern et al. [2]. Copyright 2013 by British Institute for Non-Destructive Testing).

longitudinal waves for the assessment of oxidative aging of asphalt concrete was demonstrated in Refs. [4] and [5]. Subsurface waves are bulk waves, which travel close to and parallel to the surface; the use of subsurface waves allows for interaction to occur in a plane close to the surface, allowing for a completely one-sided (i.e., top surface of the pavement) testing setup, which is truly nondestructive.

The case where two dilatational waves interact to produce a shear wave, polarized in the plane, with a difference frequency is used. The conditions necessary for interaction to occur are the following:

$$\cos[\varphi] = \left(\frac{c_L}{c_S}\right)^2 \left[1 - \frac{1}{2}\frac{\omega_1}{\omega_2}\left(1 - \frac{c_S^2}{c_L^2}\right)\left(\frac{\omega_2^2}{\omega_1^2} + 1\right)\right] \tag{3}$$

$$\tan[\gamma] = \frac{-\omega_2 \sin[\varphi]}{\omega_1 - \omega_2 \cos[\varphi]} \tag{4}$$

where φ is the angle between the two primary waves, c_L is the dilatational velocity, c_S is the shear velocity, and γ is the angle of the scattered wave relative to k_1. Dilatational transducers were mounted on variable Plexiglas angle wedges, set to 1 deg greater than the first critical angle, to generate subsurface dilatational waves, which propagate close and parallel to the surface.

As previously mentioned, the noncollinear wave mixing was first utilized to assess oxidation level in AC via a testing setup, whereby specimens were cut to the appropriate geometry so that the sensors could be incidentally mounted on the specimen faces for wave interaction at the appropriate angles. The method was then extended to be one sided by implementing variable angle wedges to generate subsurface waves. These two testing setups will now be described. For both cases, the data acquisition process was the same; only the experimental configuration was different.

3.3 Experimental Setup for Subsurface Wave Mixing. Figure 2(*a*) shows a setup for noncollinear wave mixing using incident mounted transducers, while Fig. 2(*b*) shows the setup using critically refracted longitudinal waves. For additional information, the reader is addressed to Refs. [4] and [5]. Here, critically refracted longitudinal waves, which are longitudinal bulk waves that travel nearly parallel to the free surface of a bulk medium, will be used and discussed. For this reason, they are often referred to as subsurface longitudinal waves. These two names will be used interchangeably. Longitudinal subsurface waves have the properties of bulk longitudinal waves while still being detectable at the surface [21]. Thus, subsurface waves can be employed to measure the bulk of material right below the surface where the most aging in the asphalt concrete pavement is present. Critically refracted longitudinal waves are generated at the first critical angle governed by Snell's law [21,22]

$$\frac{\sin\theta_{\text{inc}}}{c_i} = \frac{\sin\theta_L}{c_L} \tag{5}$$

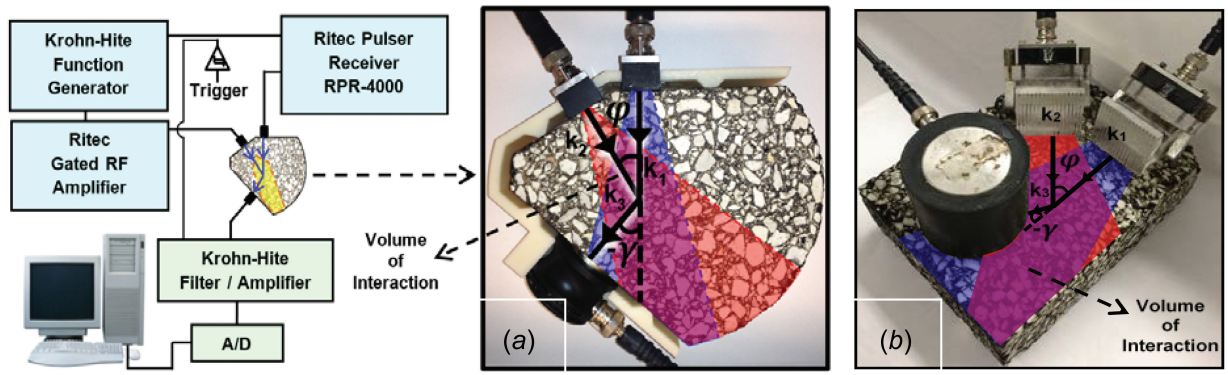

Fig. 2 Test samples schematic diagram of the ultrasonic data collection system illustrating the angle of interaction of the two longitudinal waves and the location of the receiving transducer to receive the generated scattered shear wave: (*a*) specimen cut to accommodate transducers mounted in normal incidence. The different shaded regions denote the areas of signals k_1 and k_2, respectively, due to beam spread. The region where they overlap is the volume of interaction. Note, the beam spread from k_2 is slightly higher than k_1 due to the difference in frequencies. (Reproduced with permission from McGovern et al. [4,5]. Copyright 2014 by British Institute for Non-Destructive Testing).

where c_L and c_i are the longitudinal velocities of the asphalt medium and incident wedge material, respectively, θ_{inc} is the incident angle, and $\theta_L = 90$ deg (i.e., sin $\theta_L = 1$) for the case of critical refraction, see Fig. 3.

The beam pattern of longitudinal subsurface waves was theoretically studied by Basatskaya and Ermolov [23]. They found that the beam pattern of the subsurface wave is comprised of many lobes. At the critically refracted angle, most of the energy in the main lobe is contained at the surface, but the maximum displacement occurs at an angle below the surface (e.g., ≈18 deg below the surface for steel). Note, the portion of the wave on the free surface is not purely longitudinal due to the boundary conditions (i.e., stress-free surface). When the incident angle is slightly larger than the critical angle, the main lobe becomes narrower, and the maximum displacement moves closer to the surface. As the angle is further increased beyond the critical angle, the side lobes start to dominate in amplitude over the main lobe. For incident angles slightly smaller than the critical angle, the main lobe moves away from the surface. Chaki et al. [24] verified these results via a numerical study and found that the energy of the subsurface wave is maximum at the surface for an incident angle of 1 deg greater than the first critical angle.

Figure 2(*b*) shows a schematic of the one-sided subsurface wave mixing experimental setup. Two longitudinal transducers (Panametrics V413, center frequency 500 kHz) were mounted on plastic variable angle wedges. The wedges were set at an angle such that the incident angle was 1 deg greater than the critically refracted angle for each specimen to generate subsurface longitudinal waves. The angle was measured using a digital protractor with an accuracy of 1 deg. The wedges were positioned such that the interaction angle between the two primary waves was $\varphi = 47$ deg, and both $\boldsymbol{k}_1$ and $\boldsymbol{k}_2$ propagated a distance of 8.2 cm (from the center of the angle wedge to the center of the volume of interaction) before interacting. The scattered nonlinear wave propagated a distance of 4 cm (from the center of the volume of interaction to the center of the receiving transducer face) and was received by a third longitudinal transducer (Panametrics V1011, center frequency 100 kHz), which was mounted incidentally on the surface in the path of $\boldsymbol{k}_3$ ($\gamma = -37$ deg to with respect to $\boldsymbol{k}_1$). Again, the placement of the sending/receiving transducers was based on the angles (φ and γ) calculated for the virgin specimen properties. The same transducer placement was used for all specimens. The signal generation was the same as in the incidentally mounted transducer setup. For additional information regarding the experimental setup for subsurface wave mixing, the reader is referred to the work by McGovern et al. [5–7]. Determination of the experimental setup is an iterative process, and the reader is referred to McGovern et al. [4] for details behind this process.

3.4 Data Acquisition Procedure. Data acquisition consisted of three steps: (1) operating the two sending transducers simultaneously, (2) individually operating only the first sending transducer, and (3) individually operating only the second sending transducer. To obtain the nonlinear scattered wave, i.e., the difference signal, the signals obtained from operating the sending transducers individually, i.e., one at a time, were subtracted from the signal obtained when operating the two sending transducers simultaneously. The remaining signal will now be referred as the difference signal. The difference signal, i.e., scattered shear wave, resulting from the nonlinear interaction of the two intercepting waves, is very low in amplitude due to: (1) low conversion efficiency of the interaction between the two primary dilatational waves, (2) inherent dispersion in the asphalt concrete (especially at high frequencies), and (3) the presence of the dominating, i.e., large amplitude, primary waves in the imperfect subtraction (a portion of the signal energy is lost in the conversion to the nonlinear scattered wave—this leads to the signal resulting from the addition of the signals obtained when the dilatational transducers are operated individually being larger than the signal obtained from the two longitudinal transducers are operated simultaneously). To circumvent the low amplitude and maximize the ability to detect the scattered wave, the following steps were taken: (1) a high sample rate (50 MHz) was used in order to avoid trigger jitter as suggested by Johnson and Shankland [14,15] and (2) to mitigate the scattering affects, an average of 500 waveforms was taken. For each aging level, ten independent measurements were taken.

3.5 Metrics for Oxidation Level Assessment. The two metrics used to assess the level of oxidation were the frequency at which wave interaction occurs and the efficiency of the interaction. As the frequency f_2 is swept during the data collection, the amplitude of the difference signal is continuously monitored. The frequency ratio f_2/f_1 at which the amplitude of the difference signal is maximum corresponds to the frequency ratio at which interaction takes place. This *frequency ratio* will change with material properties; hence, oxidation level as such can be used as one metric.

The nonlinear scattered wave results from interaction between the two primary waves. Accordingly, a portion of the energy of the two primary waves is used in the generation of the nonlinear wave. For this reason, the amplitude of the nonlinear scattered wave is proportional to the product of the two primary waves [11] as follows:

$$A_{age}^{(k_3)} = \beta_{age} A_{sent}^{(k_1)} A_{sent}^{(k_2)} \exp[-(\alpha^{(k_1)} + \alpha^{(k_2)})D]\exp[-\alpha^{(k3)} D_{k_3}] \quad (6)$$

where D is the propagation distance, α is the attenuation coefficient, and A denotes the amplitude of the respective primary wave. The β term is the fraction of the primary waves converted to the scattered wave and has been termed the nonlinear generation parameter. The age subscript denotes the amount of laboratory oxidative aging level (in hours). Dividing Eq. (5) by the nonlinear scattered wave amplitude of the virgin specimen and solving for β/β_0 yields

$$\frac{\beta_{age}}{\beta_0} = \left(\frac{A_{age}^{(k_3)}}{\exp[-(\alpha^{(k_1)} + \alpha^{(k_2)})D]\exp[-\alpha^{(k3)} D_{k_3}]} \right) * \left(\frac{A_0^{(k_3)}}{\exp\left[-\left(\alpha_0^{(k_1)} + \alpha_0^{(k_2)}\right)D\right]\exp[-\alpha_0^{(k3)} D_{k_3}]} \right)^{-1} \quad (7)$$

This parameter β/β_0 is termed the normalized nonlinear generation parameter, and it represents the efficiency of the nonlinear wave interaction with respect to the virgin, undamaged material.

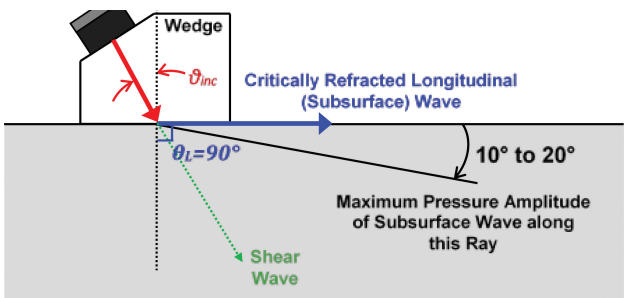

Fig. 3 Schematic of transmitted signal through angle wedge with an incident angle equal to the first critical angle to generate a critically refracted longitudinal (subsurface) wave. The main lobe has a maximum energy at the surface and a maximum pressure amplitude (i.e., displacement) along the ray 10–20 deg below the surface. (Reproduced with permission from McGovern et al. [5]. Copyright 2014 by British Institute for Non-Destructive Testing).

This parameter is the second metric for oxidation level assessment in asphalt mixtures.

3.6 Nonlinear Oxidative Damage Characterization Curve. The *nonlinear damage characterization curve* is a reference plot where f_2/f_1 is plotted versus β/β_0 for AC specimens with various levels of oxidative aging. Thus, it represents a trajectory of aging for a particular mixture in a two-dimensional space defined by the f_2/f_1 and β/β_0 parameters. The following scenario is envisioned: a practitioner can take some field measurements on the pavement and determine the level of oxidative aging of the pavement based on where the measurement(s) lie with respect to the reference curve. The pavement mixture type must be identified in order to select the appropriate curve; however, if this information is not known, measurements could be taken at the bottom of an extracted core, presuming that the bottom of the core is protected and thus shares characteristics similar to the virgin, i.e., unaged mixture.

To minimize experimental error, the nonlinear damage characterization curve should be generated in laboratory conditions by characterizing the AC specimens via the noncollinear subsurface wave mixing technique across a sufficient sample size of oxidatively aged AC specimens. Also, to minimize experimental error, the dilatational and shear velocities and corresponding attenuations should be obtained in the laboratory for the entire sample set. The dilatational velocities are used to obtain the appropriate incident angles of the wedges (1 deg above the first critical angle).

Each nonlinear damage characterization curve only needs to be generated once for a particular mixture type in the laboratory. A library of nonlinear damage characterization curves can be generated for different mixture designs, e.g., different binders, aggregate gradations, aggregate types, etc. Thus, for use in the field, all that needs to be known a priori is the type of mixture.

4 Results of Assessing Oxidative Aging

Results and conclusions regarding the development of the noncollinear wave mixing technique to assess oxidative aging will now be presented and discussed.

4.1 Nonlinear Acoustics: Noncollinear Wave Mixing. The linear acoustic results demonstrated that linear acoustic measurements, such as ultrasonic velocity, can detect high levels of oxidative aging; however, the dependence on the level of aging is not unique because more than one aging level will yield the same velocity measurement, see Fig. 1. In the work presented in this section, the nonlinear acoustic technique in the form of noncollinear wave mixing is used to assess the amount of oxidative aging present in asphalt concrete. Two parameters were used as metrics to quantify the oxidation level. One of the parameters, i.e., the frequency ratio, is inherently related to the velocity, and the other parameter, i.e., the nonlinear generation parameter, helps to circumvent the problem of nonuniqueness.

The study on noncollinear wave mixing in oxidatively aged specimens began with a feasibility study using bulk waves, whereby the specimens were cut to a geometry such that the transducers could be incidentally mounted and the waves were interacted and received at the appropriate angles as shown in Fig. 2(*a*). Of course, this geometry does not lend itself for practical implementation in the field. The action of coring and cutting a portion of AC pavement is cumbersome and ultimately not nondestructive. So, the method was extended to be one sided by employing subsurface waves. As will be shown, the results from both methods are very agreeable; therefore, the bulk of this section will focus on the results from the subsurface wave mixing studies.

To ensure that the received wave was a nonlinear wave resulting from interaction between the primary waves in the specimen, selection criteria as proposed by Johnson and Shankland [14,15] were used. Once it is verified that the nonlinear wave results from the primary wave interaction within the bulk of the sample, the data from the specimens at different aging levels could be compared. The following results will be shown for the subsurface wave case (with the wedges set to 1 deg + the critical angle).

4.2 Amplitude, Directionality, Frequency, and Time-of-Arrival Criteria. To assure that the received scattered nonlinear wave is valid, the following criteria were used: amplitude, directionality, frequency, and time of arrival.

Amplitude criterion: It was observed that as the voltage of the primary waves was increased, the amplitude of the nonlinear signal also increased in a manner proportional to the amplitudes of the primary waves.

Directionality criterion: The propagation direction of the scattered wave (i.e., γ) must match the propagation direction predicted by theory. The placement of the sensors was selected using the virgin specimens (i.e., virgin parameters) using Eqs. (3) and (4), but care was taken to minimize the difference between the virgin scattered angle γ and the scattered angle for the other "ages" to ensure that the receiving transducer was in the path of the nonlinear scattered wave for all the specimens.

Frequency criterion: To ensure that the frequency of the scattered wave matches that predicted by theory (i.e., $f_3 = f_1 - f_2$ at the appropriate f_2/f_1), the amplitude of the nonlinear scattered wave was monitored as f_2 was swept and f_1 was held constant. The maximum amplitude of the nonlinear scattered wave should occur when f_2 reaches the frequency where f_2/f_1 matches the ratio predicted by the theory. The amplitude was measured by passing the difference signal through a bandpass (30–90 kHz) filter as f_2 was swept. The selected bandpass frequency range ensured that the primary waves were filtered out as well as any very low frequencies.

Figure 4 shows a representative example of the recorded nonlinear scattered wave amplitude as f_2 was swept for the virgin specimen. The amplitude was predicted to reach a maximum when $f_2/f_1 = 0.6$ (i.e., $f_2 = 120$ kHz). The experimental data show that the amplitude reached a peak at $f_2/f_1 = 0.575$ (i.e., $f_2 = 115$ kHz), showing a 4.1% difference (i.e., 5 kHz). Theoretically, the nonlinear amplitude should only occur for a particular (i.e., theoretically predicted) frequency ratio. In reality, the

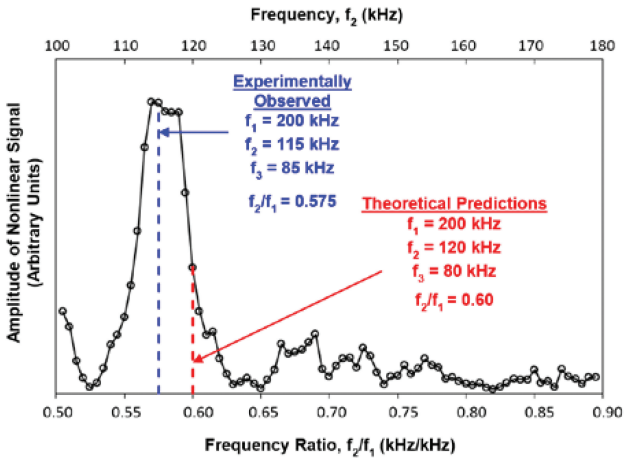

Fig. 4 Experimentally obtained amplitude of the scattered shear wave, i.e., difference signal, ($f_3 = f_1 - f_2$) as f_2 is swept from 100 kHz to 180 kHz ($f_2/f_1 = 0.50$–0.90) while f_1 is held constant at 200 kHz. This analysis was performed for all specimens to obtain the data shown in Figs. 8 and 10. The plot shown above is from the specimen oven aged for 12 h and shown as a representative case. The locations of the experimentally observed maximum and of the theoretically predicted maximum, which was obtained using the experimentally determined velocity data, and also shown for comparison. (Reproduced with permission from McGovern et al. [5]. Copyright 2014 by British Institute for Non-Destructive Testing).

nonlinear amplitude plotted as a function of the frequency ratio has a finite width. This width can most likely be to wave scattering caused by the stochastic nature of the aggregate structure, which leads to different propagation paths of the wave energy. The theory also assumes that the two interacting longitudinal waves are monochromatic and that the test sample material is isotropic and homogeneous. The deviation of the real testing conditions from theory has the effect that the nonlinear wave amplitude is spread over a range of values centered about the theoretically predicted frequency ratio. Frequency ratios at which maximum amplitude of the nonlinear signal occurred are plotted as a function of aging in Fig. 5.

Time-of-arrival criterion: To further validate that the nonlinear scattered wave was a result of nonlinear wave mixing inside the sample and not the testing apparatus, the time-domain records were examined. Nonlinearities generated by the testing equipment will have the same arrival time as the primary waves, whereas nonlinearities arriving from wave mixing in the specimen will have an arrival time corresponding to the paths dictated by the transducer placement and scattered wave angle γ (Eq. (4)). Thus, a time separation between the primary waves and the nonlinear scattered wave should exist, and experimental time of arrival should match with the theoretical time of arrival, which can be calculated assuming mean velocities and a straight ray-path analysis. Figure 6 shows the time-domain records for the specimen aged 36 h as a representative example. The time-domain records shown are for the cases when: (a) the transducers were operated simultaneously, (b) the transducers were operated individually and their time-domain records were summed, and (c) the difference between the records obtained in (a) and (b). The predicted arrival time (0.0982 ms) of the nonlinear scattered wave matched closely (≈4.7% difference) with the experimentally observed arrival time (0.1028 ms).

4.3 Nonlinear Wave Generation Parameter. Once it is determined that the difference signal has satisfied the selection criteria, the nonlinear wave generation parameter β can be computed. Figure 7 shows β for all aged specimens normalized by the average of β_0, corresponding to the virgin mixture. This normalized parameter, β/β_0, indicates the conversion efficiency of the energy transferred from the primary waves interacting to produce the scattered nonlinear wave (see Eq. (7)). Note, the stochastic nature of the asphalt concrete causes disparities in the independent measurements, as even a slight variation in the placement of the transducers can alter the travel paths of the traveling waves. It is observed that β/β_0 decreases from 0 to 24 h aging, and increases exponentially from 24 to 36 h of aging.

Since the experimental setup was based on virgin parameters, the nonlinear scattered wave will not always strike the receiving

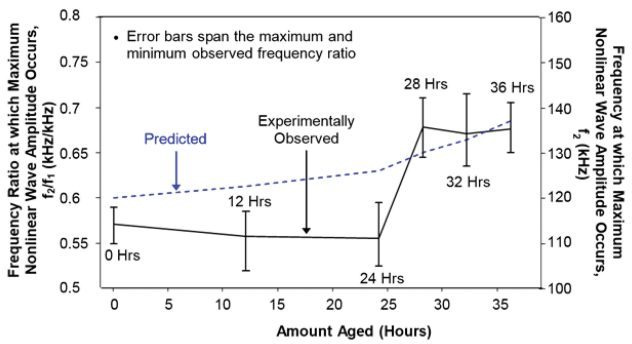

Fig. 5 Experimentally observed frequency ratio at which the maximum nonlinear scattered wave amplitude occurs. The theoretical values were predicted (see Eqs. (3) and (4)) using the experimentally obtained dilatational and shear velocities. (Reproduced with permission from McGovern et al. [5]. Copyright 2014 by British Institute for Non-Destructive Testing).

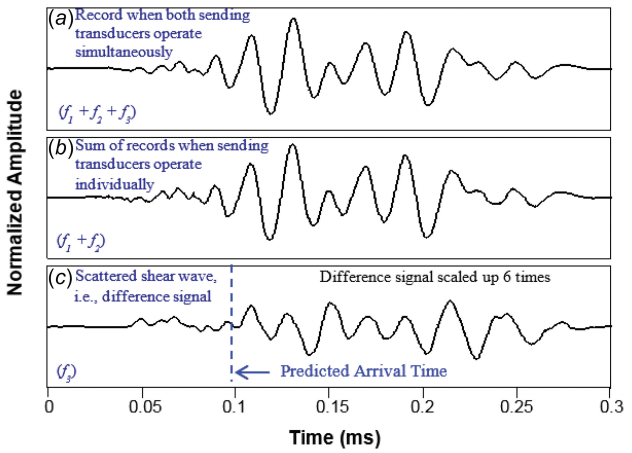

Fig. 6 Time-domain records required to obtain the nonlinear scattered shear wave: (*a*) time record obtained when both sending transducers were operated simultaneously, (*b*) time record obtained when sending transducers were operated one at a time and the received waveforms added, and (*c*) nonlinear scattered wave, i.e., the difference signal, obtained from subtracting the signals obtained from operating the sending transducers individually from the signal obtained when operating the two sending transducers simultaneously. The theoretically predicted time of arrival (0.0982 ms) for the difference signal matches closely (~4.7% difference) with the experimentally observed time of arrival (0.1028 ms). The records are all normalized by the maximum amplitude of the record in (*b*). The difference signal was scaled up six times. (Reproduced with permission from McGovern et al. [5]. Copyright 2014 by British Institute for Non-Destructive Testing).

transducer's face incidentally and in the center, because the scattered wave angle changes (i.e., increases) with the amount aged. With increased amount of aging, the nonlinear scattered wave will strike the transducer's face increasingly off-center, which may lead to an increasingly underestimate of β/β_0 with aging. The β/β_0 parameter reveals that the asphalt concrete exhibits increasingly strong nonlinear behavior with aging. This is further evidenced by

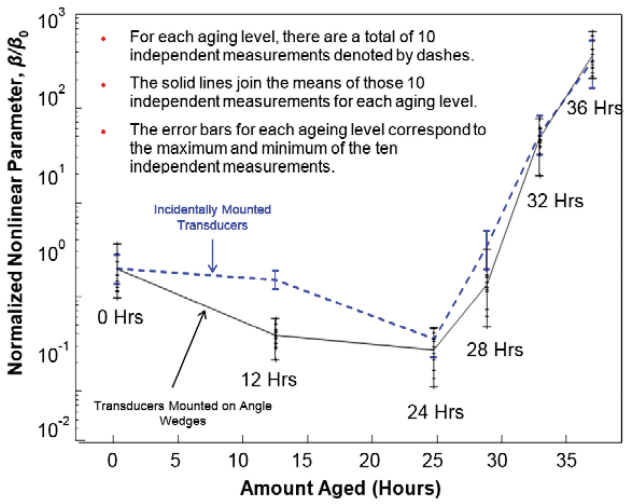

Fig. 7 Nonlinear parameter, β, versus different levels of oven aging. The parameter β is normalized with the parameter β_0, which corresponds to the virgin, i.e., unaged, mixture. The solid line represents results from the subsurface wave setup and the dashed line represents results obtained using the incidentally mounted transducer setup. (Reproduced with permission from McGovern et al. [5]. Copyright 2014 by British Institute for Non-Destructive Testing).

the fact that the nonlinear scattered wave can still be detected even with such a strong counteracting effect of attenuation.

The comparisons of the results obtained using incidentally mounted transducer, see dotted line in Fig. 7, and the results using critically refracted longitudinal waves, see solid line in Fig. 7, in the wave mixing experiments demonstrate the validity of using subsurface waves in the noncollinear wave mixing technique. The interaction angle between this study and the previous study was changed slightly to accommodate positioning of the angle wedge transducers on the finite width of the test specimen. In doing so, it is noted that the frequency ratios changed according to theory (i.e., shifted up/down). The nonlinear wave generation parameter remained nearly the same. The small observed differences are attributed to some variability during the oxidative oven-aging process of the uncompacted, i.e., lose mixtures [5]. This latter observation lends credence to the claim that the nonlinear wave generation parameter is an inherent material property, and not a function of the testing setup. The agreement of the results from these two studies indicates that subsurface waves can be used successfully to characterize oxidative aging in asphalt concrete using the noncollinear wave mixing technique.

4.4 Nonlinear Damage Characterization Curve. The measurements from Figs. 5 and 7 were used to construct the reference nonlinear damage characterization curve, which is unique for the AC mixture; refer to Fig. 8. This reference curve was used in the subsequent studies, as discussed in Sec. 5.

4.5 Extension of Nonlinear Acoustic Technique for Field Use. Recall that the subsurface noncollinear wave mixing setup required the use of variable angle wedges set to an angle of 1 deg + the first critical angle. If the linear acoustic properties are known, Snell's law can be used to determine the appropriate incident wedge angle. This can be readily done in laboratory-type conditions. Presumably, however, in the field, there is no prior knowledge of the oxidative aging level of the asphalt concrete, rendering the appropriate incident angle unknown.

Thus, the studies presented up to this point [4,5] required some knowledge of the linear acoustic properties of the AC specimens. In Refs. [6] and [7], two systematic approaches were proposed to address the issue of the unknown incident critical angle, and evidence supporting the validity of the two methods was presented. The two methods were termed the *iterative incident angle technique* and the *fixed incident angle technique*. Both methods allow the noncollinear wave mixing technique to be employed by practitioners in the field for pavement inspection, where the only pre-existing knowledge of the pavement is its mixture type.

For the iterative incident angle technique, the critical refracted angle is found iteratively. This method addresses a way to find the appropriate incident angle to generate subsurface dilatational waves, as well as a way to estimate the necessary linear parameters (i.e., velocities and attenuations) with access to only one side, i.e., the pavements surface. Once the critical refracted angle and linear parameters are found via this technique, then the subsurface noncollinear wave-mixing technique can be employed as usual.

The fixed incident angle technique was introduced to address the potentially tedious nature of iteratively determining the incident angle. This technique was developed when it was observed that one fixed incident angle could be used across the entire sample set of aged AC specimens (i.e., 0–36 h). For the mixture type and angle wedges used in this study, 73 deg was found to be the best suited angle. For a detailed discussion of the two methods, the reader is referred to Refs. [6] and [7]. Here, only the final results will be presented.

4.5.1 Iterative Incident Angle Technique. Two transducers mounted on variable angle wedges were setup in a through-transmission configuration so that one sends a square wave at the appropriate frequency (i.e., in the range of f_2 to f_1) and the other receives the signal. Both wedges were set to the same angle. The distance between the wedges was chosen sufficiently small to try to avoid any interference with bulk waves, which may have been generated via mode conversion from the wedges and reflected back from discontinuities or large inhomogeneities in the medium. The wedge angle was varied and the amplitude is recorded at each angle. When changing the angle, care was taken to not disturb the couplant conditions. The maximum of the parabola (obtained by plotting amplitude versus angle) corresponds to the ideal incident angle to use in the testing setup. This angle subtracted by 1 deg corresponds to the first critical angle.

Once the ideal incident angle was found, the velocity and attenuation of the mixture was found via Snell's law. The dilatational attenuations were found by using through-transmission subsurface waves over a range of frequencies. To measure the shear wave attenuation, subsurface shear waves were not used due to uncertainty in how the stress-free surface boundary condition affects the propagation and detection of the shear wave. Instead, an empirical relation between the shear attenuation and the longitudinal velocities for oxidatively aged AC specimens was found using data obtained from a previous study. Refer to Ref. [6] for details on this process.

Noncollinear wave mixing was then performed using the iteratively found angles and the testing setup described previously. This experimental study was performed in a "blind study" format, whereby it was assumed that no prior knowledge of the linear acoustic properties of the AC specimen existed. For each sample, the frequency ratio f_2/f_1 at which the nonlinear scattered wave amplitude was greatest was recorded. The normalized wave generation parameter β/β_0 was found for each specimen using the recorded amplitudes and estimated attenuations as described in Refs. [6] and [25]. The average of five independent measurements for each specimen is superimposed as x's on the laboratory determined nonlinear characterization curve in Fig. 9(*a*). It is observed that the blind study measurements follow closely the nonlinear characterization curve.

4.5.2 Fixed Incident Angle Technique. A blind study was again performed (in a similar fashion discussed in the previous section). Figure 9(*b*) contains the results from the blind study, where these measurements are denoted as "x's." As expected, the specimens with the lowest amounts of aging (0–24 h) deviate the most from the laboratory determined reference curve due to the large deviations in the first critical angle with respect to the incident angle.

The biggest advantage of using the fixed incident angle technique over the iterative incident angle technique is the ease at which it can be implemented, rendering it ideal for field use. However, there are drawbacks in terms of its accuracy. Although the f_2/f_1 ratio metric does not suffer using this method, the estimation of the β/β_0 parameter suffers due to relative larger errors in the attenuation estimates [7]. Another drawback to fixed angle technique is that although the chosen incident angle may be ideal for a small range of aged specimens, it is not the best possible angle for generating subsurface longitudinal waves for the entire aged sample set. Furthermore, for other AC mixture types, more than one incident angle may be necessary to achieve a wide range of aging assessment. Finally, since the most suitable incident angle is not necessarily being used, multiple peaks in the frequency ratio versus amplitude curve may be detected, which may complicate the analysis [7].

4.6 Fracture Performance of Aged Asphalt Mixtures From Nonlinear Acoustic Measurements. While it was shown that the nonlinear acoustic metrics can detect the level of oxidation present in pavements, nothing was reported about the relationship of the nonlinear acoustic metrics to thermal and mechanical properties of the asphalt mixtures. Once taking nonlinear acoustic measurements, practitioners will likely desire to use these measurements to infer the pavement's mechanical response, such as fracture resistance. This information is of

practical importance, and hence work was also carried out [26] to quantify the relationship between nonlinear acoustic metrics and the embrittlement temperatures and mechanical fracture properties using an acoustic emission approach [27–29] and the disk-shaped compact tension test [8,30–32], respectively. The embrittlement temperatures of asphalt mixtures obtained using acoustic emission test are also presented in Fig. 10(*a*). Results show that embrittlement temperature of asphalt mixtures progressively get warmer with increasing aging. The higher the aging level of mixture, the warmer the onset of the thermally induced microdamage in the asphalt concrete samples. Figure 10(*b*) shows the average DC(T) fracture energies of asphalt mixtures at different aging levels (0–36 h) [26]. Figure 10(*c*) shows the average DC(T) fracture energies of asphalt mixtures at different aging levels (0–36 h) versus the normalized nonlinear generation parameter [26]. Figures 11(*a*) and 11(*b*) illustrate the relationship between the nonlinear acoustic metrics and the fracture energy and embrittlement temperatures, respectively, in the mixtures. Good relationships exist among the nonlinear acoustic metrics, the mixtures fracture energy and the embrittlement temperatures, which because of space limitations are not presented here. For additional information, the readers are referred to Ref. [26].

5 Rejuvenators

Upon determination of the level of oxidative aging in the pavement, engineers may decide to take preventative or corrective measures. The ability to monitor the oxidation level of the pavement subsequent to taking corrective action is necessary to assess the effectiveness of the action(s) as well as aid in making future decisions toward preserving the pavement. In particular, asphalt rejuvenation products were used as the corrective action, as they have recently received much attention in the pavement community for their relative ease and speed of application. Thus, the natural extension to this work is to investigate the feasibility of using the noncollinear wave-mixing technique to assess the effectiveness of rejuvenation products as a corrective action, which entailed studying the efficacy of rejuvenation products themselves.

Asphalt rejuvenators are asphalt additives and modifiers which aim to revitalize, provide sealing, and restore the physical and chemical properties of the aged asphalt concrete [33]. Rejuvenators address the issue of oxidative hardening by softening the aged asphalt binder through restoration of the asphaltenes-to-maltenes ratio [34]. After applying a thin layer of rejuvenator over the top surface of pavement, the rejuvenator penetrates the tortuous porous structure of the AC mixture via gravity and capillary action, and diffuses through the asphalt concrete to chemically react with the asphalt binder. The rejuvenator/binder reaction restores the binder's material properties to its original state. The asphalt binder is thus softened, increasing its adhesive properties so that the asphalt concrete is less susceptible to thermal and mechanical cracking.

As described by Brown [35], with the exception of visual inspection, there is no standardized method to evaluate the

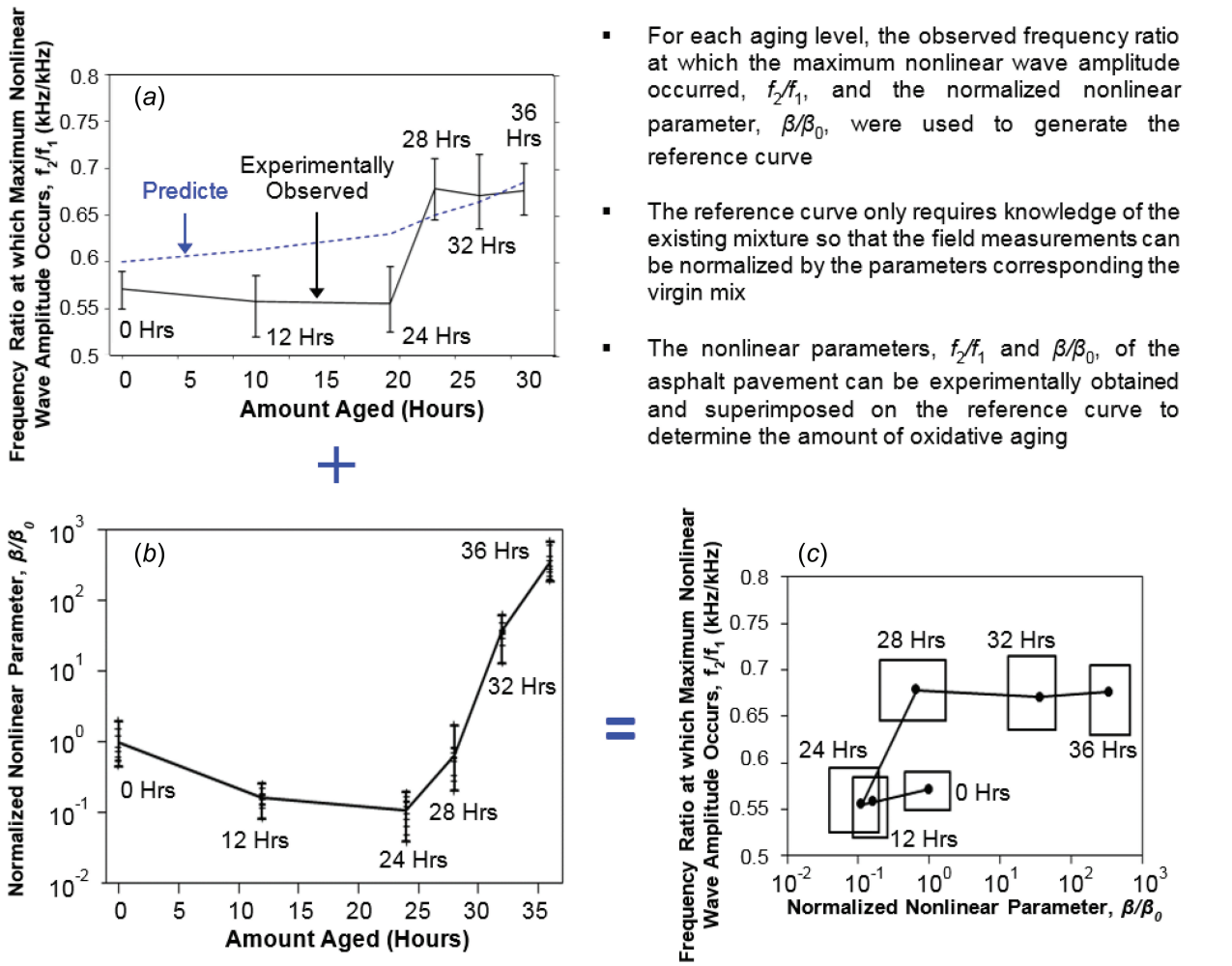

Fig. 8 Generation of the reference curve, i.e., the frequency ratio versus the normalized nonlinear parameter. The data from (*a*) and (*b*) is used to create (*c*). (Reproduced with permission from McGovern et al. [25]. Copyright 2015 by American Society for Nondestructive Testing).

performance of rejuvenators. Currently, the ability of rejuvenators to improve pavements' durability is typically evaluated by: (1) estimating the penetration in samples at 25 °C using asphalt binder extracted from untreated and treated cores; (2) comparing the viscosity at 60 °C of asphalt binder samples extracted from untreated and treated cores; and (3) comparing the percentage of aggregate loss when untreated and treated samples are subjected to a pellet abrasion test. Mainly because these tests are cumbersome and time consuming, they are not often used. There exists a need for a more reliable method for determining the effectiveness of rejuvenating agents.

In this section, a study on the effectiveness of rejuvenators to restore the material properties of the aged asphalt back to its original state is presented. This chapter begins with a summary of the experimental investigations and a discussion of the results. Then, the efficacy of the rejuvenation product, Reclamite, was studied using the noncollinear wave mixing technique. This chapter will conclude with a blind study, which was performed using the fixed incident angle technique to demonstrate its potential for field use.

5.1 Materials and Experimental Procedures. The material preparation and experimental procedures will now be outlined for the noncollinear wave mixing tests used in the asphalt rejuvenator studies.

5.1.1 Noncollinear Wave Mixing: Setup and Material Preparation. A set of gyratory compacted asphalt specimens was created with a mix design of 5.9% (by weight of total mixture) PG 64-22 binder with a 4% air void content. Prior to compaction, the loose mixtures were oven aged for a total of 36 h at 135 °C. To encourage uniform aging throughout the specimen, the loose mixture was hand stirred every 12 h. A gyratory compactor was used to compact the loose mixture into cylinders. Rectangular specimens were then cut from the gyratory specimens with dimensions $150 \times 175 \times 50$ mm. Rejuvenator was applied to upper face of each specimen, in the amount of 10% of the binder (by weight). Each rejuvenator coated specimen was left to dwell for a specific amount of time: 3–6 days in 1 day increments, 1–8 weeks in 1 week increments, and 12 weeks for a total of 13 test specimens with different dwell time periods. Once the dwell time reached the desired amount, the specimen was wiped of any excess

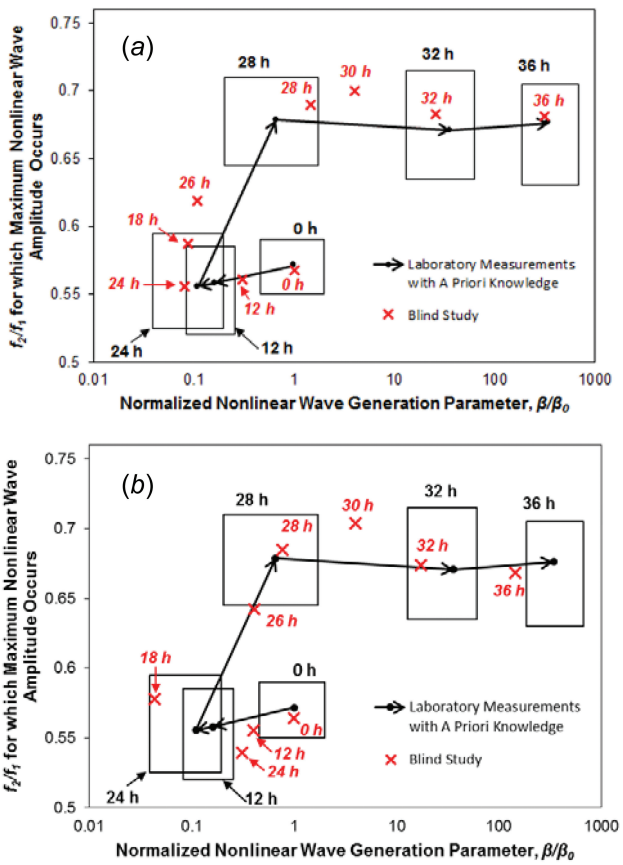

Fig. 9 Results from the "blind study" superimposed on the nonlinear damage characterization curve where the *x*'s represent the average of five measurements taken from the top surface without any prior knowledge of the specimen aging (only the type of mixture was known): (*a*) via the iterative incident angle technique and (*b*) via the fixed incident angle technique (Reproduced with permission from McGovern et al. [6,7]. Copyright 2015 and 2016 by British Institute for Non-Destructive Testing and Elsevier Publishing)

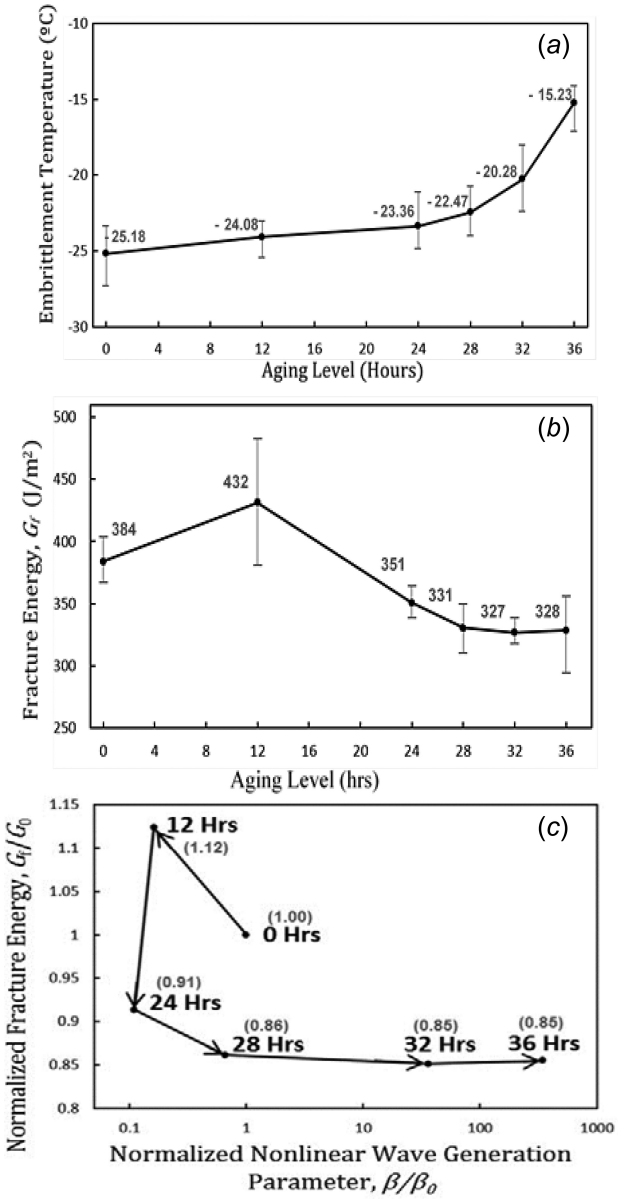

Fig. 10 Thermal and mechanical properties of asphalt mixtures at different aging levels: (*a*) acoustic emission embrittlement temperatures of asphalt mixtures at different aging levels (0–36 h), (*b*) average DC(T) fracture energies of asphalt mixtures at different aging levels (0–36 h), and (*c*) normalized fracture energy versus normalized nonlinear wave generation parameter for increasing levels of oxidative damage. The measured fracture energy values are also shown within parenthesis. (Reproduced with permission from McGovern et al. [26]. Copyright 2017 by Transportation Research Board).

rejuvenator, to improve couplant conditions, and immediately ultrasonically tested. The specimens were weighed before and after wiping the rejuvenator to determine how much rejuvenator was removed during the wiping process. The noncollinear wave mixing testing setup was the iterative incident angle technique.

5.2 Rejuvenator Efficacy. To assess the efficacy of the rejuvenation product, Reclamite, testing using the noncollinear wave mixing approach was carried out.

5.2.1 Noncollinear Wave Mixing Results. Prior to implementing the noncollinear wave mixing technique, the optimal incident angle was found experimentally. The experimentally observed optimal angles (refer to Fig. 12) were found to vary with the rejuvenator dwell time. In a previous study, the optimal angle for a virgin specimen (i.e., no rejuvenator or oxidative aging) was found as 51 deg, and the optimal angle for a specimen aged 36 h (with no rejuvenator) was found as 73 deg. For specimens with a dwell time of 3–5 days, the optimal angle approached the virgin optimal angle with each successive day. For the specimens with a dwell time greater than 5 days, the optimal angles varied about the virgin optimal angle within a ±7 deg range. These angles were all observed to be closer to the angle corresponding to the virgin sample than that of the 36 h, indicating that the rejuvenator may be having a restorative effect on the aged specimens. For the specimens with a dwell time greater than 5 days, largest difference (14.7% difference with respect to the virgin angle of 51 deg) corresponded to the sample with a dwell time of 6 weeks, which had an experimentally determined optimal angle of 44 deg. It is interesting to note that the samples with 5, 7, and 8 weeks dwell time had incident angles of 56 deg (55 deg for the 7 week sample), which was larger than the virgin incident angle. This might suggest that the oxidative damage was not fully reversed. It is possible that the rejuvenator did not penetrate as thoroughly as in the other samples, leaving areas of unaffected binder.

Noncollinear wave mixing with subsurface dilatational waves was also carried out in the usual fashion for each specimen using the experimentally determined optimal incident angle. The difference signal was checked against the selection criteria to verify that it was a result of the primary wave interaction and not the testing equipment. The f_2/f_1 and β/β_0 were determined for each specimen and plotted on the reference nonlinear damage characterization curve. Refer to Fig. 12(*a*), which shows selected data from some of the rejuvenator coated specimens superimposed on the reference curve. Not all of the data was plotted to facilitate viewing. It was observed that past 4 weeks of dwell time, the samples have f_2/f_1 and β/β_0 values which fall within error of the nonlinear parameters for the virgin specimen.

For the specimen with a dwell time of 8 weeks, there was a large amount of excess rejuvenator which was wiped off. This may explain why the nonlinear parameters deviated from the

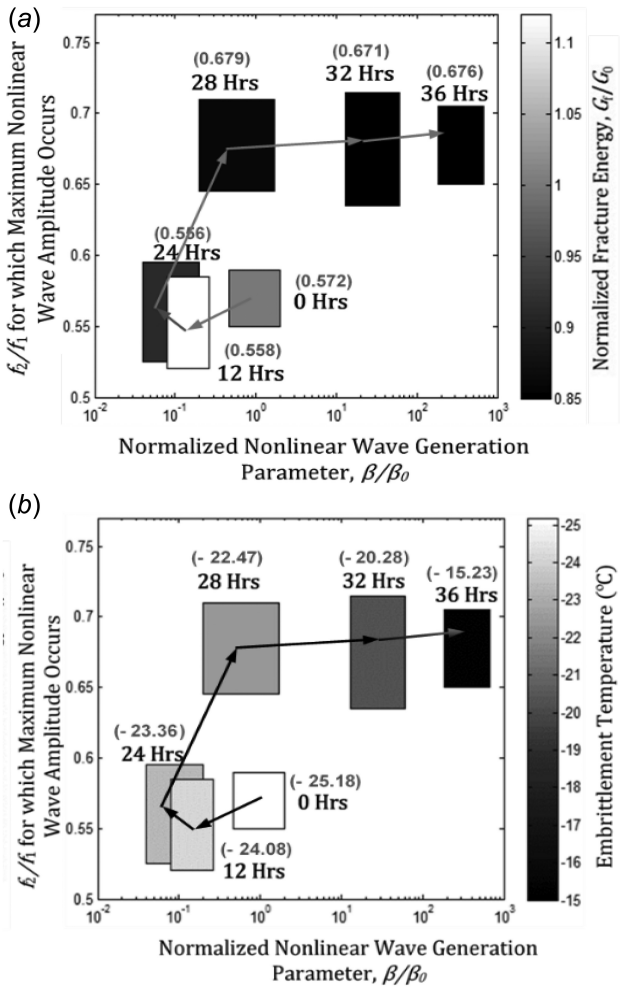

Fig. 11 Evolution of the normalized fracture energy (*a*) and of embrittlement temperatures (*b*) with the evolution of oxidative aging damage and their relationship with the nonlinear acoustic parameters. The measured fracture energy and the embrittlement temperature values are within parenthesis. (Reproduced with permission from McGovern et al. [26]. Copyright 2017 by Transportation Research Board).

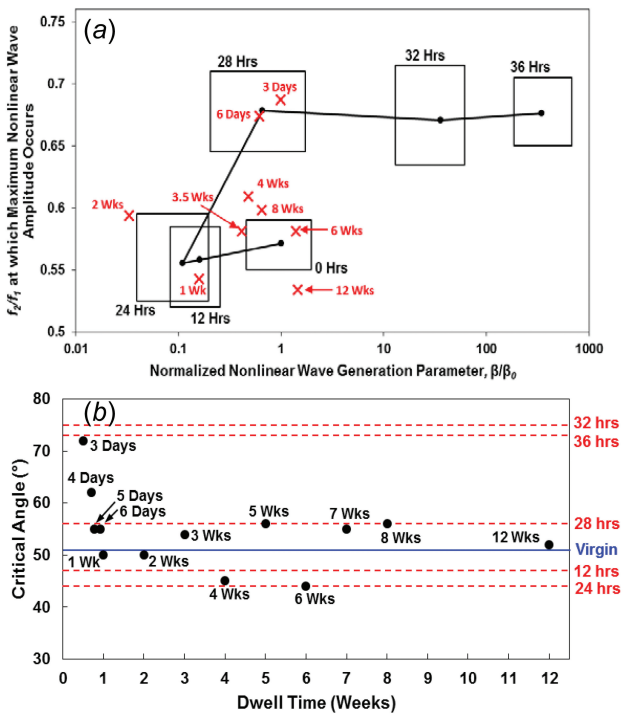

Fig. 12 Use of rejuvenators on 36 h aged specimens using the iterative angle technique: (*a*) the frequency ratio f_2/f_1 at which maximum amplitude of the nonlinear wave occurs versus the nonlinear wave generation parameter β, normalized by the virgin β_0, where the average of five nonlinear measurements of the rejuvenator-coated specimens (shown as *x*'s) are superimposed on the reference curve denoted in black and (*b*) experimentally measured critical angles for samples with different dwell times. The solid line indicates the critical angle for a reference virgin specimen (no rejuvenator). The dashed lines indicate the critical angles for specimens subjected to various amounts of aging with no rejuvenator for comparison purposes. (Reproduced with permission from McGovern et al. [25]. Copyright 2015 by American Society for Nondestructive Testing).

virgin nonlinear parameters further than the specimens with a lower dwell time of 5 and 6 weeks. For the specimens with a dwell time of 4 weeks and under, the nonlinear parameters deviated further from the virgin parameters in a manner that may be correlated with the dwell time. From 1/2 to 4 weeks, the nonlinear parameters become closer to the virgin parameters with each successive week. This is in agreement with the AE results shown in Sec. 4.6 (Fig. 10(*a*)), and indicates that the rejuvenator takes time to chemically act on the aged binder.

Figure 13 shows some representative selected data that were used to find the f_2/f_1 values. Recall, f_2/f_1 was found by holding f_1 constant, monitoring the amplitude of $\boldsymbol{k}_3$ ($f_3 = f_1 - f_2$) as f_2 is swept, and determining the point at which $\boldsymbol{k}_3$ reaches maximum. Figure 13(*a*) shows the amplitude of $\boldsymbol{k}_3$ as f_2 was swept for a few selected samples. For some samples (e.g., the samples with dwell times of 4 days, 1 week, and 2 weeks), the process was relatively straightforward: the peak amplitude was located with respect to the f_2/f_1 ratio. However, presence of multiple peaks in some samples served to complicate the analysis (e.g., the samples with dwell times of 6 days, 4 weeks, 6 weeks, and 8 weeks). Multiple peaks can occur due to nonuniformity of the rejuvenator penetration. Furthermore, the nonlinear interaction occurs over a finite volume, see Fig. 2. Within this volume, the rejuvenator does not necessarily penetrate and act on the binder in a uniform matter, which may result in pockets of unaffected, aged binder, and pockets of rejuvenated binder. Thus, interactions will occur at different f_2/f_1 ratios, since the binder properties vary with location within the interaction region. For a detailed examination of Fig. 13, the authors are referred to McGovern et al. [7].

5.2.2 Use of Rejuvenator as Corrective Action. The efficacy of the asphalt rejuvenation product was demonstrated using the noncollinear wave mixing studies. Once the rejuvenator was determined to be a viable option for corrective action, the field applicable version of the noncollinear wave mixing technique, the fixed incident angle technique was also employed in Ref. [36] to test the feasibility of using such a technique in the field to monitor the efficacy of the rejuvenator on the pavement as a corrective action. These results will now be briefly presented and discussed.

The material preparation and experimental setups were the same as described before. The fixed incident angle technique was used for the test procedure. A blind study was carried out in a similar fashion as before where no prior knowledge of the specimen acoustic properties was assumed. Once the nonlinear parameters, f_2/f_1 and β/β_0, of the AC specimens were recorded, they were plotted against a reference plot to determine the effective level of oxidative aging. Figure 14(*a*) shows the average of five (f_2/f_1, β/β_0) measurements for the samples exposed to rejuvenator for a prescribed amount of dwell times [36]. The measurements (denoted by crosses) are superimposed on the corresponding reference plot for the mixture used in this study, which is denoted by the solid black lines. Note that the reference plot is only valid for the particular AC mix design for which it was generated and using a fixed angle.

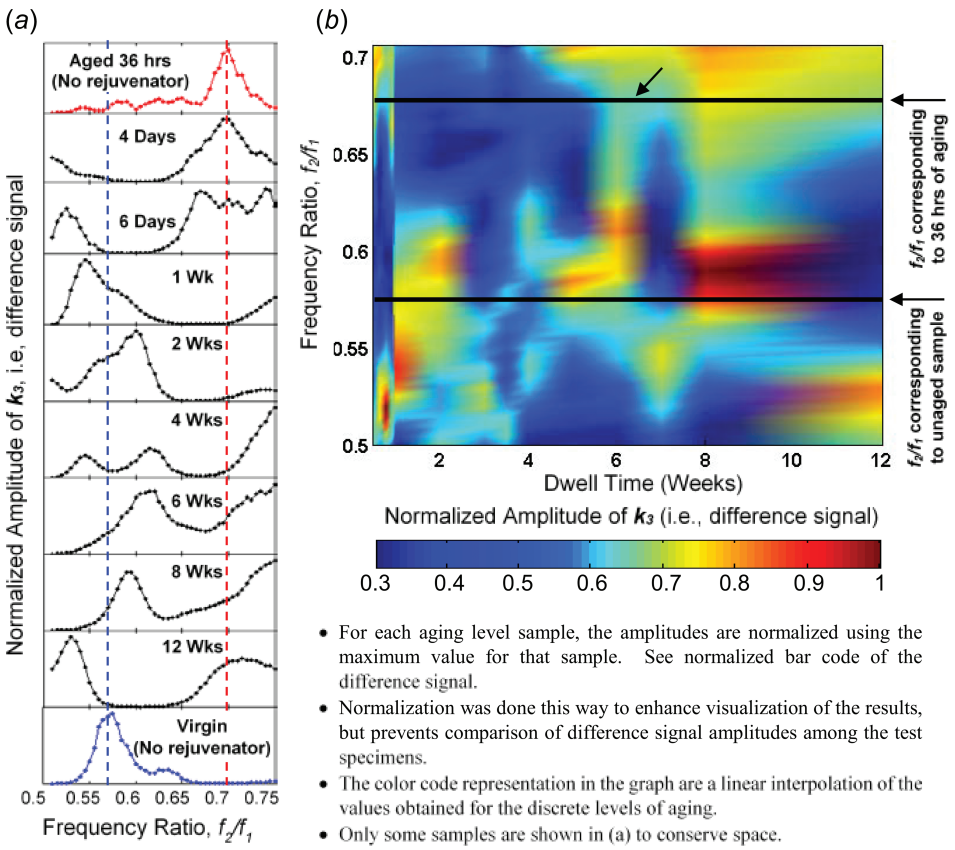

Fig. 13 (*a*) and (*b*) shows the normalized amplitude (A) of the scattered wave with respect to the dwell time and frequency ratio f_2/f_1, where (*b*) depicts A as a color/shades of gray code in the axis perpendicular to the plane. For each sample, these amplitudes are normalized using the maximum value for that sample; see normalized bar code of the difference signal. This was done to enhance visualization of the results, but prevents comparison of the difference signal amplitudes among the test specimens. The color/shades of gray code representation in the graph are a linear interpolation of the values obtained for the different samples. Note that at each dwell time, the color/shades of gray code is normalized from 0 to 1. (Reproduced with permission from McGovern et al. [25]. Copyright 2015 by American Society for Nondestructive Testing).

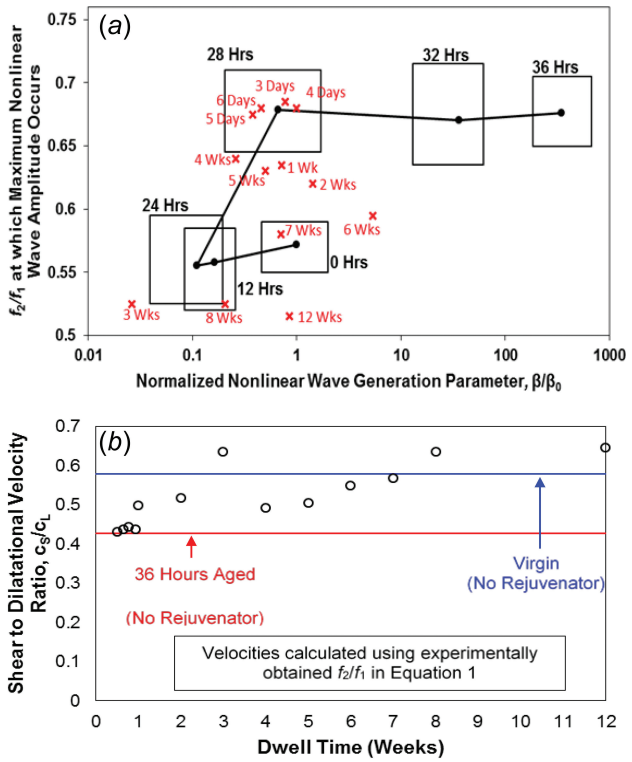

Fig. 14 Use of rejuvenators on 36 h aged specimens using the fixed angle technique: (*a*) damage evolution path due to increased levels of oxidative oven-aging (solid line and solid dots) using a fixed angle technique, as well as the average of five measurements taken on specimens aged 36 h exposed to rejuvenator for increasing amount of dwell times (crosses) and (*b*) velocity ratio, c_S/c_L, for each dwell time as determined by the experimentally measured frequency ratios, f_2/f_1. The solid lines denote the values for specimens with no rejuvenator aged 0 h, i.e., virgin, and 36 h, respectively. (Reproduced with permission from McGovern and Reis [36]. Copyright 2016 by Transportation Research Board).

For specimens with a dwell time of 0–7 weeks, it was generally observed that the specimen exhibited nonlinear properties (f_2/f_1, β/β_0) increasingly closer to that of virgin specimens with an increase in the dwell time. Beyond 7 weeks, the specimen properties also exhibited properties, which correspond to a binder with a lower stiffness than the virgin binder. This can be seen in Fig. 14(*b*), which shows the velocity ratio, c_S/c_L, as a function of the dwell time. The velocity ratios were computed by plugging the experimentally obtained frequency ratios into Eq. (3) and solving for the positive root. The softening of the binder has a stronger effect on the dilatational velocity because the stiffness associated with the shear velocity also depends upon the aggregates interlocking.

6 Conclusions

Noncollinear wave mixing techniques geared toward addressing the need for a nondestructive method to evaluate the ability of asphalt concrete pavement surfaces to resist channeling crack forms, such as thermal and block cracking, are presented and discussed. The research work presentation follows a natural trajectory, starting with an investigation of the effects of oxidative aging on the linear acoustic properties (i.e., velocities and attenuations) of asphalt concrete. Then, after a feasibility study was performed, where test samples were cut to the appropriate geometry to allow for incident mounting of the transducers for bulk wave mixing, critically refracted longitudinal waves were used to assess oxidative damage from the pavement surface. This nonlinear acoustic technique was then extended to be applicable for field use by modifying the setup to be one sided so that all measurements could be taken from the pavement surface, including the linear measurements. Finally, the developed method was then used to assess the efficacy of maintenance treatments such as rejuvenators in restoring the asphalt concrete to its original crack resistance state. Here, it was observed that the use of rejuvenators has the effect of restoring thermal and mechanical property values of oxidized pavements to those values corresponding to virgin pavements after a sufficient amount of dwell time.

Acknowledgment

The authors are grateful for the technical support of Dr. George Vansteenburg. The authors are also grateful for the technical support of Dr. Jeb S. Tingle (ERDC-RDE-GSL-MS). The authors are also very grateful to the American Society for Nondestructive Testing, the British Institute for Non-Destructive Testing, Elsevier, and the Transportation Research Board for the permission to reproduce figures, as acknowledged in the figure captions.

Funding Data

- The U.S. Airforce Civil Engineering Center (AFCEC) (Contract No. W912HZ-16-C-0006).

References

[1] Petersen, J., 2009, "A Review of the Fundamentals of Asphalt Oxidation," Transportation Research Board, Washington, DC, Transportation Research Circular No. E-C140.
[2] McGovern, M., Behnia, B., Buttlar, W., and Reis, H., 2013, "Characterization of Oxidative Aging in Asphalt Concrete—Part 1: Ultrasonic Velocity and Attenuation Measurements and Acoustic Emission Response Under Thermal Cooling," Insight, **55**(11), pp. 596–604.
[3] McGovern, M., Behnia, B., Buttlar, W., and Reis, H., 2013, "Characterization of Oxidative Aging in Asphalt Concrete—Part 2: Estimation of Complex Moduli," Insight, **55**(11), pp. 605–609.
[4] McGovern, M., Buttlar, W., and Reis, H., 2014, "Characterization of Oxidative Aging in Asphalt Concrete Using a Non-Collinear Ultrasonic Wave Mixing Approach," Insight, **56**(7), pp. 367–374.
[5] McGovern, M., Buttlar, W., and Reis, H., 2014, "Estimation of Oxidative Aging in Asphalt Concrete Pavements Using Non-Collinear Wave Mixing of Critically Refracted Longitudinal Waves," Insight, **57**(1), pp. 25–34.
[6] McGovern, M., Buttlar, W., and Reis, H., 2015, "Field Estimation of Oxidative Aging in Asphalt Concrete Pavements Using Non-Collinear Wave Mixing," Insight, **57**(11), pp. 625–634.
[7] McGovern, M., Buttlar, W., and Reis, H., 2016, "Field Assessment of Oxidative Aging in Asphalt Concrete Pavements With Unknown Acoustic Properties," J. Constr. Build. Mater., **116**, pp. 159–168.
[8] Braham, A. F., Buttlar, W. G., Clyne, T. R., Marasteanu, M. O., and Turos, M. I., 2009, "The Effect of Long-Term Laboratory Aging on Asphalt Concrete Fracture Energy," J. Assoc. Asphalt Paving Technol., **78**, pp. 417–454.
[9] Murnaghan, F. D., 1951, *Finite Deformation of an Elastic Solid*, Wiley, New York.
[10] Landau, L. D., and Lifshitz, E. M., 1959, *Theory of Elasticity*, Addison-Wesley Publishing, Reading, MA.
[11] Jones, G., and Kobett, D., 1963, "Interaction of Elastic Waves in an Isotropic Solid," J. Acoust. Soc. Am., **35**(1), pp. 5–10.
[12] Rollins, F., Taylor, L., and Todd, P., 1964, "Ultrasonic Study of Three-Phonon Interactions—II: Experimental Results," Phys. Rev., **136**(3A), pp. A597–A601.
[13] Taylor, L., and Rollins, F., 1964, "Ultrasonic Study of Three-Phonon Interactions—I: Theory," Phys. Rev., **136**(3A), pp. A591–A596.
[14] Johnson, P., and Shankland, T., 1989, "Nonlinear Generation of Elastic Waves in Granite and Sandstone: Continuous Wave and Travel Time Observations," J. Geophys. Res., **94**(B12), pp. 17729–17733.
[15] Johnson, P., Shankland, T., Connell, O. R., and Albright, J., 1987, "Nonlinear Generation of Elastic Waves in Crystalline Rock," J. Geophys. Res., **92**(B5), pp. 3597–3602.
[16] Korneev, D. A., 2014, "Possible Second-Order Nonlinear Interactions of Plane Waves in an Elastic Solid," J. Acoust. Soc. Am., **135**(2), pp. 591–598.
[17] Zarembo, L. K., and Krasil'nikov, V. A., 1971, "Nonlinear Phenomena in the Propagation of Elastic Waves in Solids," Sov. Phys., **13**(6), pp. 778–797.
[18] Gol'dberg, Z. A., 1960, "Interaction of Plane Longitudinal and Transverse Elastic Waves," Sov. Phys. Acoust., **6**(3), pp. 306–310.
[19] McCall, K. R., 1994, "Theoretical Study of Nonlinear Elastic Wave Propagation," J. Geophys. Res., **99**(B2), pp. 2591–2600.
[20] Hughes, D. S., and Kelly, J. L., 1953, "Second-Order Elastic Deformation of Solids," Phys. Rev., **92**(5), pp. 1145–1149.

[21] Bray, D., and Stanley, R., 1997, *Nondestructive Evaluation: A Tool in Design, Manufacturing, and Service*, CRC Press, New York.
[22] Kinsler, L., Frey, A., Coppens, A., and Sanders, J., 1984, *Fundamentals of Acoustics*, 3rd ed., Wiley, New York.
[23] Basatskaya, L., and Ermolov, I., 1981, "Theoretical Study of Ultrasonic Longitudinal Subsurface Waves in Solid Media," Sov. J. Nondestr. Testing, **16**, pp. 524–530.
[24] Chaki, S., Ke, W., and Demouveau, H., 2013, "Numerical and Experimental Analysis of the Critically Refracted Longitudinal Beam," Ultrasonics, **53**(1), pp. 65–69.
[25] McGovern, M., Farace, N., Buttlar, W., and Reis, H., 2015, "Effectiveness of Rejuvenators on Aged Asphalt Concrete Using Ultrasonic Non-Collinear Subsurface Wave Mixing," Mater. Eval., **73**(10), pp. 1365–1376.
[26] McGovern, M., Behnia, B., Buttlar, W., and Reis, H., 2017, "Estimation of Fracture Performance of Aged Asphalt Mixtures From Nonlinear Acoustic Measurements," J. Transp. Res. Board, **2631**, pp. 11–19.
[27] Apeagyei, A., Buttlar, W., and Reis, H., 2009, "Assessment of Low-Temperature Embrittlement of Asphalt Binders Using an Acoustic Emission Approach," Insight, **51**(3), pp. 129–136.
[28] Behnia, B., Dave, E., Buttlar, W., and Reis, H., 2016, "Characterization of Embrittlement Temperature of Asphalt Materials Through Implementation of Acoustic Emission Technique," J. Constr. Build. Mater., **111**, pp. 147–152.
[29] Sun, Z., Behnia, B., Buttlar, W. G., and Reis, H., 2016, "Acoustic Emission Quantitative Evaluation of Rejuvenators to Restore Embrittlement Temperatures to Oxidized Asphalt Mixtures," Constr. Build. Mater., **126**, pp. 913–923.
[30] Dave, E. V., Behnia, B., Ahmed, S., Buttlar, W. G., and Reis, H., 2011, "Low Temperature Fracture Evaluation of Asphalt Mixtures Using Mechanical Testing and Acoustic Emissions Techniques," J. Assoc. Asphalt Paving Technol., **80**, pp. 193–220.
[31] Hill, B., Oldham, D., Behnia, B., Fini, E. H., Buttlar, W. G., and Reis, H., 2013, "Low Temperature Performance Characterization of Bio-Modified Asphalt Mixtures Containing Reclaimed Asphalt Pavement," Transp. Res. Rec., **2371**(1), pp. 49–57.
[32] ASTM, 2007, "Standard Test Method for Determining Fracture Energy of Asphalt Concrete-Aggregate Mixtures Using the Disk-Shaped Compact Tension Geometry," American Society of Testing Materials, West Conshohocken, PA, Standard No. ASTM 7313-07.
[33] Shen, J., Amirkhanian, S., and Miller, J., 2007, "Effects of Rejuvenating Agents on Superpave Mixtures Containing Reclaimed Asphalt Pavement," J. Mater. Civ. Eng., **19**(5), pp. 376–384.
[34] García, Á., Schlangen, E., and Van de Ven, M., 2011, "Properties of Capsules Containing Rejuvenators for Their Use in Asphalt Concrete," Fuel, **90**(2), pp. 583–591.
[35] Brown, E., 1988, "Preventative Maintenance of Asphalt Concrete Pavements," Transp. Res. Rec., **1**, pp. 6–11.
[36] McGovern, M. E., Buttlar, W. G., and Reis, H., 2016, "Nondestructive Field Evaluation of Aging Levels of Rejuvenated Asphalt Concrete Pavements," J. Transp. Res. Board, **2576**, pp. 1–9.